microrotation fields (3), (4). The total macroscopic load, however, is the same at the end, which may be arbitrarily far from the region of interest. The different stress distributions at the end in fields (3) and (4) are therefore equivalent in the sense of Saint-Venant. In this sense, the case $N=0$ is pathological. For some specific problems, the solution for $N=0$ is found to coincide with the solution for classical elasticity. This case is not equivalent to classical elasticity, however; the microstructural degrees of freedom remain. Classical elasticity is recovered as a special case of micropolar elasticity only if α, β, γ, and κ all vanish.

A physical example that exhibits some features of the situation just considered is as follows. Consider a long rod of a composite material made of parallel stiff fibers embedded in a compliant matrix. Fiber orientation is random, so macroscopic properties are isotropic. The spatial average of force per unit area upon fibers and matrix may be regarded as the force stress, and the corresponding spatial average of couple upon each individual fiber, per unit area, may be regarded as the couple stress. At each end of the rod, we may macroscopically twist the end by a given angle, and microscopically twist the end of each fiber in the opposite direction until the net end torque is zero. If the interface between fiber and matrix is perfectly lubricated, the effect of the end displacements and rotations may be expected to propagate an arbitrary distance down the rod. This situation is analogous to the continuum case $N=0$ considered in the foregoing. Significant end effects may also occur in classical elasticity of highly anisotropic materials [9]; by contrast the preceding example depends on micromechanical degrees of freedom rather than anisotropy.

Micropolar elasticity has been found to be useful in the interpretation of recent experiments upon solids with fibrous [10] and cellular [11] structures. Nonzero values of N were inferred from these experiments. No structures corresponding to the preceding physical example, however, were studied.

To conclude, the special case $N=0$ in micropolar elasticity is pathological in that specification of the macroscopic end load on a rod does not uniquely determine the displacement and microrotation fields far from the end. The dependence of these fields on remote, localized distributions of self-equilibrated load calls into question the applicability of Saint-Venant's principle for such solids.

References

1 Eringen, A. C., "Theory of Micropolar Elasticity," in: *Fracture*, Liebowitz, M., ed., Vol. 2, Academic Press, New York, 1968, pp. 621-729.

2 Cowin, S. C., "An Incorrect Inequality in Micropolar Elasticity Theory," *J. Appl. Math, Phys. (ZAMP)*, Vol. 21, 1970, pp. 494-497.

3 Krishna Reddy, G. V., and Venkatasubramanian, N. K., "On the Flexural Rigidity of a Micropolar Elastic Circular Cylinder," ASME JOURNAL OF APPLIED MECHANICS, Vol. 45, 1978, pp. 429-431.

4 Mindlin, R. D., and Tiersten, H. F., "Effects of Couple Stresses in Linear Elasticity," *Arch. Rat. Mech. Anal.*, Vol. 11, 1962, pp. 415-448.

5 Gauthier, R. D., and Jahsman, W. E., "A Quest for Micropolar Elastic Constants," ASME JOURNAL OF APPLIED MECHANICS, Vol. 42, 1975, pp. 369-374.

6 Willson, A. J., "The Micropolar Elastic Vibrations of a Circular Cylinder," *Int. J. Eng. Sci.*, Vol. 10, 1972, pp. 17-22.

7 Gauthier, R. D., and Jahsman, W. E., "Bending of a Curved Bar of Micropolar Elastic Material," ASME JOURNAL OF APPLIED MECHANICS, Vol. 43, 1976, pp. 502-503.

8 Gauthier, R. D., "Experimental Investigations on Micropolar Media," in: *Mechanics of Micropolar Media*, Brulin, O., and Hsieh, R. K. T., eds., World Scientific, Singapore, 1982.

9 Horgan, C. O., "On Saint-Venant's Principle in Plane Anisotropic Elasticity," *J. Elasticity*, Vol. 2, 1972, pp. 169-180.

10 Yang, J. F. C., and Lakes, R. S., "Experimental Study of Micropolar and Couple Stress Elasticity in Bone in Bending," *J. Biomechanics*, Vol. 15, 1982, pp. 91-98.

11 Lakes, R. S., "Experimental Microelasticity of Two Porous Solids," *Int. J. Solids and Structures*, in press.

Effect of Debonding on the Stability of Fiber-Reinforced Composites

J. Barber[1] and N. Triantafyllidis[1]

1 Introduction

In this work we present some analytical solutions to a model problem in order to elucidate the effects of a preexisting debonding between fiber and matrix on the stability properties of reinforced composites.

Our analysis is motivated by some recent experimental [1] and theoretical investigations [2, 3] on delamination buckling of fiber-reinforced and laminated composites subjected to compressive loads along the reinforcing direction. Of particular interest is the effect of the debonded length on the critical buckling load which is investigated here for two extreme cases of the fiber-to-matrix relative stiffness. By ignoring fiber interaction effects and using a simple model for our problem, we are able to obtain closed-form analytical solutions.

More specifically, we consider a beam on two elastic type foundations. The effect of debonding in a certain region is modeled by the local exclusion of tensile lateral forces. Realistic buckling loads and eigenmodes have been found for all the cases considered and all critical loads were of the same order of magnitude as that for the fully bonded composite. Our results at this stage are preliminary in nature, but they indicate the possibility of solution of some more complicated but more realistic delamination buckling problems.

2 Fiber Buckling in a Soft Matrix

To study the effects of debonding in the fiber buckling of a soft matrix composite, the matrix material on each side of the fiber is idealized as an elastic foundation of modulus k. Two cases will be considered. In the first case the entire fiber is assumed to be debonded from the matrix material so that tensile stresses at the matrix-fiber interface are nowhere allowed. In the second case debonding will be assumed only in a finite zone of length $2a$.

2.1 Fully Debonded Fiber (Debonded Zone $-\infty \le x \le +\infty$). In the case of full debonding, every point of the fiber will be in contact with one of the two foundations (the one corresponding to a compressive distrbuted load). Consequently, the problem is equivalent to the buckling (under a lateral force P) of a continuous beam resting on only one elastic foundation of modulus k. The critical load for this case is well known (see, for example, Timoshenko and Gere [4]) and is

$$P_d = (4\ k\ EI)^{1/2} \tag{2.1}$$

where EI is the fiber's bending stiffness. For the fully bonded fiber, of course, both the elastic foundations on each side of the fiber will be active at buckling, and the total effective foundation stiffness will be $2k$. Therefore the corresponding lateral buckling load P_b should be given by

$$P_b = (8\ K\ EI)^{1/2} \tag{2.2}$$

For the partially bonded fiber to be analyzed subsequently, the corresponding critical load P_p is expected to satisfy $P_d \le P_p \le P_b$.

2.2 Partially Debonded Fiber (Debonded Zone $-a \le x \le a$). If $u(x)$ is the lateral displacement of the fiber due to

[1] Department of Mechanical Engineering and Applied Mechanics, and Department of Aerospace Engineering, respectively, The University of Michigan, Ann Arbor, Mich. 48109.

Manuscript received by ASME Applied Mechanics Division, August, 1984.

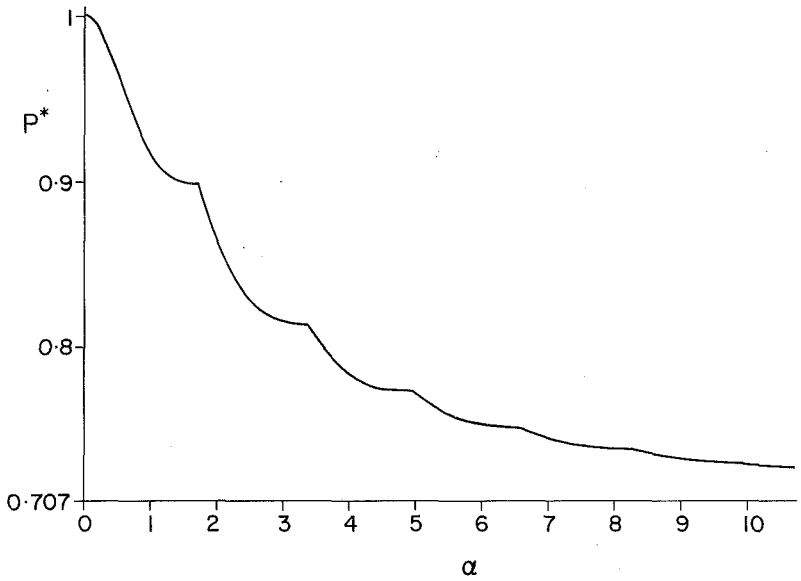

Fig. 1 Nondimensionalized load P^* versus crack length parameter α for a partially debonded fiber in a soft matrix

an axial load P_p, the governing equation for the fiber buckling is

$$EI\frac{d^4u}{dx^4}+P_p\frac{d^2u}{dx^2}+ku=0 \quad \text{in debonded zone} \quad |x|\le a$$
$$EI\frac{d^4u}{dx^4}+P_p\frac{d^2u}{dx^2}+2\,ku=0 \quad \text{in bonded zone} \quad |x|\ge a \tag{2.3}$$

As mentioned earlier, only solutions in the range $P_d \le P_p \le P_b$ are of interest here, and thus the general solutions to (2.3) can be put in the form

$$u(x)=\begin{cases} [C_1^- \cos(\omega(x-a))+C_2^- \sin(\omega(x-a))] \\ \exp(-\lambda\,(x-a)): x\ge a \\ A_1^- \sin(\omega_1(x-a))+A_2^- \sin(\omega_2(x-a)) \\ +A_1^+ \sin(\omega_1(x+a))+A_2^+ \sin(\omega_2(x+a)): \ |x|\le a \\ [C_1^+ \cos(\omega(x+a))+C_2^+ \sin(\omega(x+a))] \\ \exp(\lambda(x+a)): x\le -a \end{cases} \tag{2.4}$$

where ω_1, ω_2, ω, λ, and P^* are given by

$$\left.\begin{aligned} \omega_1&=(P^*+(P^{*2}-\tfrac{1}{2})^{1/2})^{1/2}(2k/EI)^{1/4}, \\ \omega_2&=(P^*-(P^{*2}-\tfrac{1}{2})^{1/2})^{1/2}(2k/EI)^{1/4} \\ \omega&=((1+P^*)/2)^{1/2}(2k/EI)^{1/4}, \\ \lambda&=((1-P^*)/2)^{1/2}(2k/EI)^{1/4}, P^*=P_p/P_b \end{aligned}\right\} \tag{2.5}$$

The eight continuity conditions (four at $x=+a$ and four at $x=-a$) for $u(x)$ and its first three derivatives – following from the displacement, slope, moment and shear continuity requirements for the fiber – provide a linear homogeneous system of eight equations for the eight unknowns A_i^+, A_i^-, C_i^+, C_i^- $(i=1,2)$. After considerable manipulations one can show that a nontrival solution to the aforementioned system is possible if and only if

$$F(\lambda,\omega,\omega_1,\omega_2;\ \tan(.))F(\lambda,\omega,\omega_1,\omega_2;-\cot(.))=0 \tag{2.6}$$

where $F(\lambda,\omega,\omega_1,\omega_2;g(.))$ is given by

$$\begin{aligned} F \equiv\ & 2\lambda(\omega_2^2-\omega_1^2)(\lambda^2+\omega^2+\omega_1\omega_2 g(\omega_1 a)g(\omega_2 a)) \\ & +\omega_1 g(\omega_1 a)(\omega_1^2(\lambda^2+\omega^2) \\ & +\omega_2^2(\omega^2-3\lambda^2)-(\lambda^2+\omega^2)^2-\omega_1^2\omega_2^2) \\ & +\omega_2 g(\omega_2 a)(\omega_1^2\omega_2^2+(\lambda^2+\omega^2)^2 \\ & -\omega_2^2(\lambda^2+\omega^2)-\omega_1^2(\omega^2-3\lambda^2)) \end{aligned} \tag{2.7}$$

It can also be shown that $F(\ldots;\tan(.))=0$ corresponds to a symmetric eigenmode while $F(\ldots;\ -\cot\ (.))=0$ corresponds to an antisymmetric one with respect to the origin $x=0$.

The results giving the lowest value of P^* satisfying (2.6) as a function of $\alpha\equiv a(k/EI)^{1/4}$ (a properly nondimensionalized debonded zone size) are presented in Fig. 1. Note that, for fixed material properties, as the zone size α increases from 0 (fully bonded fiber) to ∞ (fully debonded fiber), the nondimensionalized critical load P^* decreases montonically from 1 to $1/\sqrt{2}=0.707$.

3 Fiber Buckling in a Stiff Matrix

In the previous solution, the contact region(s) between the fiber and the matrix extend over a full half wave of the bifurcation eigenmode. In practice, a much more restricted contact area is anticipated in view of the nonlocal pressure-displacement relation for the elastic matrix. A limiting case of some interest is that in which the contact area is sufficiently localized for the pressure exerted by the matrix to be considered as a system of point forces. This will be the case if the stiffening effect of adjacent fibers is sufficiently weak for rigid body displacement of the matrix to dominate the localized elastic deformation. The problem can then be idealized as an elastic beam constrained between two parallel rigid beams on elastic foundations. The magnitude of each (normal) point force on the fiber is proportional to the local displacement and to the wavelength of the corresponding buckling mode say $4a$ i.e.,

$$F=4\,a\,k\,u(a) \tag{3.1}$$

with $u(a)$ the eigenmode's maximum amplitude.

It is sufficient to consider the governing (buckling) equation for one quarter wavelength, namely

$$EI\frac{d^2u}{dx^2}+P(u)=Fx/2 \quad 0\le x\le a \tag{3.2}$$

with boundary conditions

$$u=0 \quad \text{at} \quad x=0, \quad \frac{du}{dx}=0 \quad \text{at} \quad x=a \tag{3.3}$$

For no interpenetration between fiber and support, u is additionally required to satisfy

$$\frac{d^2u}{dx^2} < 0 \quad \text{at} \quad x = a \tag{3.4}$$

The solution to (3.2), and (3.3) is thus found to be

$$u(x) = Fx/2P - F\,a\,\sin(\eta x/a)/2P\eta\,\cos\,\eta; (\eta \equiv a(P/EI)^{1/2}) \tag{3.5}$$

which, upon taking into consideration (3.1) and (3.4) yields

$$P/P_b = [\eta(\eta - \tan\eta)]^{1/2}/2, \quad \text{with} \quad (2n-1)\pi \le \eta \le n\pi;\ n \epsilon I\!N \tag{3.6}$$

One can easily show from (3.6) that the minimum possible buckling load P corresponds to an η-satisfying

$$2\eta = \tan 2\eta,\ \pi/2 < \eta < \pi \quad \text{i.e.,} \quad \eta = 2.2467$$

and hence the corresponding critical value for the nondimensionalized critical load is $P^* = P/P_b = 1.4008$ (almost twice the value of the fully debonded fiber in the soft matrix $P^* = 0.707$).

4 Conclusions

In an attempt to investigate the effects of fiber debonding on the critical load for delamination-type buckling in fiber-reinforced composites, we have constructed some simpler models for sparingly reinforced composites under plane strain conditions. It was found that the buckling load varies between 1.4008 and 0.707 of that for the fully bonded fiber, with the upper limit corresponding to a highly rigid matrix and the lower one corresponding to a very soft matrix. These preliminary results indicate that considerable critical load variations can occur in a fiber-reinforced composite, depending on the fiber to matrix relative stiffness, and on the size of the debonded zone.

References

1 Knauss, W. B., Babcock, C. D., and Chai, H., "Visualization of Impact Damage of Composite Plates by Means of the Moire Technique," NASA-CR 159261, Apr. 1980.

2 Chai, H., Babcock, C. D., and Knauss, W. G., "One Dimensional Modelling of Failure in Laminated Plates by Delamination Buckling," *Int. J. Solids Structures*, Vol. 17, 1981, pp. 1069–1083.

3 Bottega, W. J., and Meawall, A., "Delamination Buckling and Growth in Laminates," ASME JOURNAL OF APPLIED MECHANICS, Vol. 50, 1983, pp. 184–189.

4 Timoshenko, S. P., and Gere, J. M., *Theory of Elastic Stabililty*, 2nd ed., McGraw-Hill, New York, 1961.

Crack Growth Prediction of Subsurface Crack in Yielded Material

D. Y. Tzou[1] and G. C. Sih[2]

1 Introduction

The problem of wear delamination by the growth of a subsurface crack subjected to compressive and shear loading was discussed in [1]. The objective of this Note is to show that the direction of crack growth can be determined by application of the strain-energy density criterion even though the surroundiong material undergoes plastic deformation.

In what follows, the subsurface crack problem will be resolved by application of the incremental theory of plasticity and the strain-energy density criterion. The modified version of the PAPST finite element program [2] will be used to determine the first increments of crack growth at the left and right tips of the crack. The values of the strain-energy density function dW/dV at the nodes and Gaussian points in Fig. 1 are first obtained. The Lagrangian method of interpolation is then applied to find the stationary values of dW/dV. Referring to the finite element grid pattern in Figs. 1 and 2, 1/9 and 4/9 intermediate nodes are introduced at elements adjacent to the crack tips ensuring the required $1/r$ singularity of the strain-energy density field[3]. The physical dimensions and loads in Fig. 2 correspond to those in [1]. Outlined in Table 1 are the material properties with the available critical strain-energy density $(dW/dV)_c^*$ defined as

$$\left(\frac{dW}{dV}\right)_c^* = \left(\frac{dW}{dV}\right)_c - \left(\frac{dW}{dV}\right)_p \tag{1}$$

in which $(dW/dV)_p$ pertains to that portion of the energy density dissipated by plastic deformation being no longer available during the growth of macrocrack. The variations of dW/dV as a function of θ are calculated for a fixed radius of $r \simeq 0.25$ μm centered at the right and left tips of the crack. Displayed graphically in Fig. 3 are the results. Note that the dW/dV curves indeed possess minima near $\theta = 0$ deg. They correspond to crack initiation angles of approximately 6 deg at the right tip and 0 deg at the left tip. According to the strain-energy density criterion [3], which remains valid when yielding occurs, the subsurface crack extends almost parallel

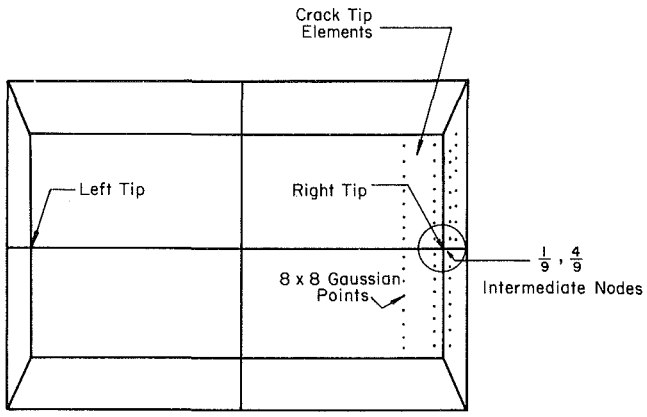

Fig. 1 Crack tip elements and Gaussian points

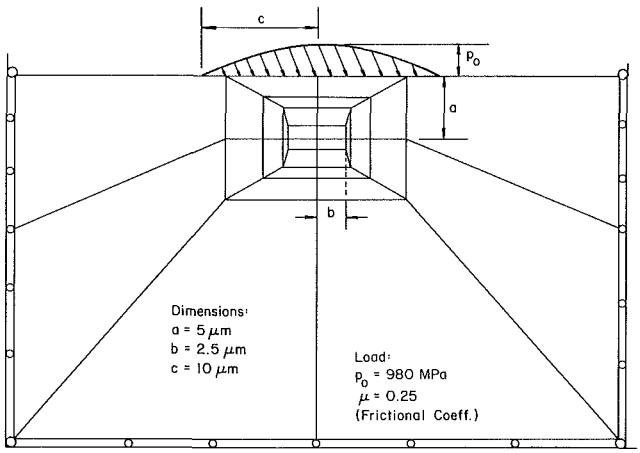

Fig. 2 Finite element grid pattern and load applied

Table 1 Mechanical properties of material in subsurface crack problem

Young's modulus E (MPa)	Tangent modulus E_T (MPa)	Poisson's ratio ν	Critical available strain-energy density $(dW/dV)_c^*$ (MPa)
1.96×10^5	19.6	0.28	1.638

[1] Research Assistant, Department of Mechanical Engineering and Mechanics, Lehigh University, Bethlehem, Pa. 18015.

[2] Professor of Mechanics and Director of Institute of Fracture and Solid Mechanics, Lehigh University, Bethlehem, Pa. 18015. Fellow, ASME

[3] The $1/r$ singular behavior of the strain energy density function holds for all material and is independent of loading and crack type.

Manuscript received by ASME Applied Mechanics Division, August, 1984.